Microsyst Technol (2015) 21:263–276
DOI 10.1007/s00542-014-2186-8

TECHNICAL PAPER

Design of experiments based factorial design and response surface methodology for MEMS optimization

M. M. Saleem · A. Somá

Received: 30 September 2013 / Accepted: 15 April 2014 / Published online: 13 May 2014

Abstract This paper presents the application of the design of experiments technique based factorial designs and response surface methodology (RSM) for optimization of MEMS devices. The RSM methodology is used to optimize the geometric parameters of the symmetric toggle RF MEMS switch to minimize the switch pull-in voltage. Fractional factorial based Plackett–Burman screening design is developed and the corresponding pull-in voltage is obtained, through finite element method (FEM) based simulations, for different combinations of the dimensional parameters. Analysis of variance is performed to distinguish the most significant parameters affecting the output response. The significant parameters, obtained using Plackett–Burman screening design, are further investigated using second order Box–Behnken design to obtain the optimal levels of the significant parameters and analyze their interactions. Regression analysis is carried out to check the adequacy of the Box–Behnkan based response surface model for predicting the output response. The effect of the significant parameters and their interactions on the pull-in voltage is analyzed through model based 3D surface and contour plots. The optimal levels of the parameters for a pull-in voltage ≤15 V, with compact device dimensions, are determined and verified through FEM simulations. A comparison is made for the results obtained through RSM with the analytical results presented in the literature. This showed a close agreement, verifying the practicability of this approach for the optimization of MEMS devices.

M. M. Saleem (✉) · A. Somá
Department of Mechanical and Aerospace Engineering,
Politecnico di Torino, Turin, Italy
e-mail: mubasher.saleem@polito.it

A. Somá
e-mail: aurelio.soma@polito.it

1 Introduction

RF MEMS switches have been widely used for different applications. The major advantages of the RF MEMS switches are low power consumption, good electrical performance, high linearity and high level of the integration as compared to other solid state devices (Rebeiz 2003; Bouchaud and Knoblich 2007; Rebeiz et al. 2009). However, high actuation voltage, switching speed, low RF power handling capability and reliability are still the major limitations that designers have to consider (Giacomozzi et al. 2008). To overcome these issues recently a new device design, called "symmetric toggle switch" (STS), based on the push-pull mechanism has been proposed (Rangra et al. 2005; Maninder et al. 2009; Farinelli et al. 2008). Lowering the electrostatic pull-in voltage of STS switch has always been a major concern of RF MEMS switch designers. High actuation voltage leads to the charge injection which strongly affects the long term reliability of the capacitive switches.

Major goal of a MEMS designer is to develop optimal configuration of a device, given a set of performance and constraint guidelines. Traditionally, this goal is achieved by developing analytical design models (Mukherjee et al. 1998; Benmessaoud and Nasreddine 2013; Pramanik et al. 2006), FEM modeling (Wang and Liu 2009; De Pasquale et al. 2010; Wan and Lowther 2007; Ballestra et al. 2008), artificial neural networks (Lee and Filipovic 2005; Lee et al. 2006) and genetic algorithms (Wilcock and Kraft 2011; Zhang et al. 2005; Liu et al. 2012). These methods though serve the purpose to certain extent, but their inconvenience for complex designs and high computational cost rises the need for the alternative optimization approaches. Design of experiments (DOE) based design optimization explores the design space of a device, at different sample

points, in an efficient manner thus reducing the computational cost and helping to analyze and optimize the complex geometries. DOE approach is used to study the effects of one or more factors on single or multiple output responses. In general, full factorial design approach is most efficient and allows all factorial effects to be estimated independently with $2^{(k)}$ experimental runs, where k is the number of factors. In practice, a full factorial design is often not desirable because of its lack of run size economy as the number of factors increases. Generally, certain higher order interactions are negligible so fractional factorial designs (FFD), using only a fraction of the full factorial design, are used to study the factorial main effects and low order interactions (Montgomery 1997). FFDs are denoted by $2^{(k-p)}$ where p is the fraction of the design to be constructed.

FFDs are classified into two major groups: regular designs and non-regular designs. Regular designs are obtained by defining relations among factors (Hamada and Wu 2000; Box and Draper 1987). These designs are limited in choices of run size because they must be powers of two. Non-regular designs such as Plackett–Burman designs (Plackett and Burman 1946), help to alleviate this problem by allowing for better management of run size economy. Additionally, these designs are available in run sizes that are multiples of four giving more flexibility in analyzing different number of factors at different levels. As fewer degrees of freedom are available in FFDS, some factors are aliased (biased) with each other and for non-regular designs this aliasing is more complex. However, for screening designs where goal is to identify the significant main factors effect on the output response rather than factor interactions, non-regular Plackett–Burman designs provide a good alternative to full factorial or fractional factorial regular designs.

Proper choice of a design is very important in any response surface investigation. Important characteristics for a good design are discussed by Box and Draper (1987). First order models are mostly used for the important factors screening purposes while second order models are used to study the detailed effect of the factors on the output response. Most frequently used second order designs are 3^k factorial design, central composite design (CCD) and the Box–Behnken design (BBD). Comparison between BBD and other response surface designs has shown that the BBD and Doehlert matrix are slightly more efficient than CCD but much more efficient than the 3^k factorial designs (Ferreira et al. 2007). Efficiency of an experimental design is defined as the number of coefficients in the estimated model divided by the number of experiments. The number of the experimental runs required for the development of BBD is defined as $N = 2k(k-1) + C_0$ as compared to 3^k for factorial design and $N = 2^k + 2k + C_0$ for CCD where k is the number of factors and C_0 is the number of central points.

In this paper, Sect. 2 describes briefly the working principle of the STS RF MEMS switch design. Section 3 explains the DOE based optimization methodology. Plackett–Burman screening design and ANOVA are used to screen out the most significant factors affecting the output response i.e. pull-in voltage. ANOVA assumptions are validated prior to performing the analysis. Significant factors are further investigated using RSM in Sect. 4. Box–Behnkin based design is implemented and a second order metamodel is developed to predict and optimize the output response. The results obtained are discussed and validated in Sect. 5.

2 Symmetric toggle switch working principle

Rangra et al. (2005) and Farinelli et al. (2008) have presented STS RF MEMS switch designs. These designs are based on the push-pull mechanism, fabricated through FBK-irst MEMS process using gold structural layer. Figure 1 shows the schematic diagram and working principle of the symmetric toggle micromachined switch. The inner and outer pairs of the actuation electrodes of the two microactuators are electrically shortened by polysilicon lines and are called “pull-in” and “pull-out” electrodes respectively. The pull-in electrodes when biased to a voltage greater than the pull-in threshold voltage, bring the center area of the beam in contact with the oxide layer on the transmission line. This results the switch in off-state. The switch is in on state when the voltage is applied on the pull-out electrodes.

3 Experimental design and statistical analysis

3.1 Placket–Burman screening design

The design variables (control factors) considered for the design optimization, as shown in Fig. 1, are top electrode length (TEL), top electrode width (TEW), torsion spring length (TSL), torsion spring width (TSW), connecting lever length (CLL), connecting lever width (CLW), central bridge length (CBL) and central bridge width (CBW). At the early design optimization stage, Placket–Burman design is used to screen out the most important factors affecting the output response. It is assumed that the important main effects will be much larger than the two factor interactions. Each factor is coded at two levels, -1 for the low level and the $+1$ for the high level. The control factor low and high levels and their respective codes are shown in Table 1.

3.2 FEM based electromechanical analysis

The pull-in voltage, for different combinations of the control factors, is obtained using *ANSYS*^{TM} based FEM simulations.

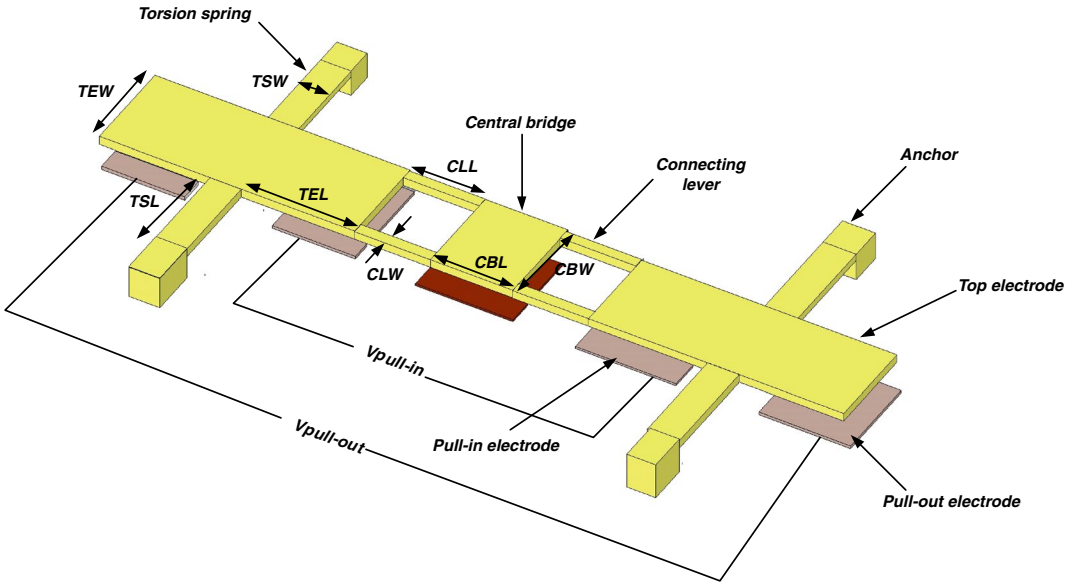

Fig. 1 Schematic of the symmetric toggle RF MEMS switch

Table 1 Control factors levels and their respective codes

Code	Control factor	Low level (−1) (μm)	High level (+1) (μm)
X_1	*TEL*	100	150
X_2	*TEW*	100	150
X_3	*TSL*	30	60
X_4	*TSW*	10	20
X_5	*CLL*	30	60
X_6	*CLW*	10	20
X_7	*CBL*	100	150
X_8	*CBW*	100	150

Structural parts are modeled by using Shell 63 elements. Poisson ratio $\upsilon = 0.42$, Young's modulus of 98.5 GPa and specific density of $19.32 \times 10^{-15} \frac{\text{kg}}{\mu\text{m}^3}$ for gold are assumed. As the electrical and mechanical domains are directly coupled in electrostatic analysis, so electromechanical coupling between the two domains is modeled using transducer elements (TRANS 126). These elements take on the form of a lumped element with voltage and structural DOFs as the cross variables and current and force as through variables. Electrostatic mesh is removed from the problem domain and is replaced by a set of TRANS 126 using EMTGEN macro, attached to top electrode, providing a reduced order modeling of a coupled electrostatic-structural system. To simplify, it is assumed that the residual stress on the gold membrane is zero and damping is negligible.

Table 2 shows the Placket–Burman design matrix with 12 runs and the corresponding output response i.e pull-in voltage obtained through FEM simulations. With the exception of the first row, which consists of all +1s, every column is the same as the one prior with every point shifted one point down until the cycle is completed.

3.3 Analysis of variance for Placket–Burman design

Analysis of variance (ANOVA) is carried to study the effect of the control factors $(X_1, X_2, X_3, X_4, X_5, X_6, X_7, X_8)$ on the output response. ANOVA assumes that the sources of variability in the response variable can be attributed to the factors as well as to the random noise. This analysis helps to determine: (1) which factor have the significant effect on the response (2) how much variability in response is attributed to each factor.

3.3.1 Mean models and factor level effect

For the y_{ij} being the jth response in the ith control factor level for any factor, the separate mean model is given as (Montgomery 1997):

$$y_{ij} = \mu_i + \epsilon_{ij} = \begin{cases} i = 1, 2, \ldots a \\ j = 1, 2, \ldots n \end{cases} \quad (1)$$

Where μ_i is the mean response for the ith factor level, a is the number of factor levels, n is the number of times the factor level appears in the design and ϵ_{ij} are the errors that are independently and normally distributed. For the single mean model each factor level is assumed to have the same mean equal to overall mean μ. For single mean Eq. 1 becomes;

$$y_{ij} = \mu + \epsilon_{ij} \quad (2)$$

Montgomery (1997) and Mason et al. (2003) have shown that $\mu_i = \mu + \alpha_i$, where α_i is the ith factor level effect,

Table 2 Plackett–Burman design matrix and corresponding pull-in voltage for each run

Run no.	X_1	X_2	X_3	X_4	X_5	X_6	X_7	X_8	Pull-in voltage (V)
1	+1	+1	+1	+1	+1	+1	+1	+1	18.5
2	−1	+1	−1	+1	+1	+1	−1	−1	48.0
3	−1	−1	+1	−1	+1	+1	+1	−1	32.0
4	+1	−1	−1	+1	−1	+1	+1	+1	36.0
5	−1	+1	−1	−1	+1	−1	+1	+1	32.8
6	−1	−1	+1	−1	−1	+1	−1	+1	38.4
7	−1	−1	−1	+1	−1	−1	+1	−1	57.8
8	+1	−1	−1	−1	+1	−1	−1	+1	22.5
9	+1	+1	−1	−1	−1	+1	−1	−1	23.2
10	+1	+1	+1	−1	−1	−1	+1	−1	15.4
11	−1	+1	+1	+1	−1	−1	−1	+1	31.8
12	+1	−1	+1	+1	+1	−1	−1	−1	21.0

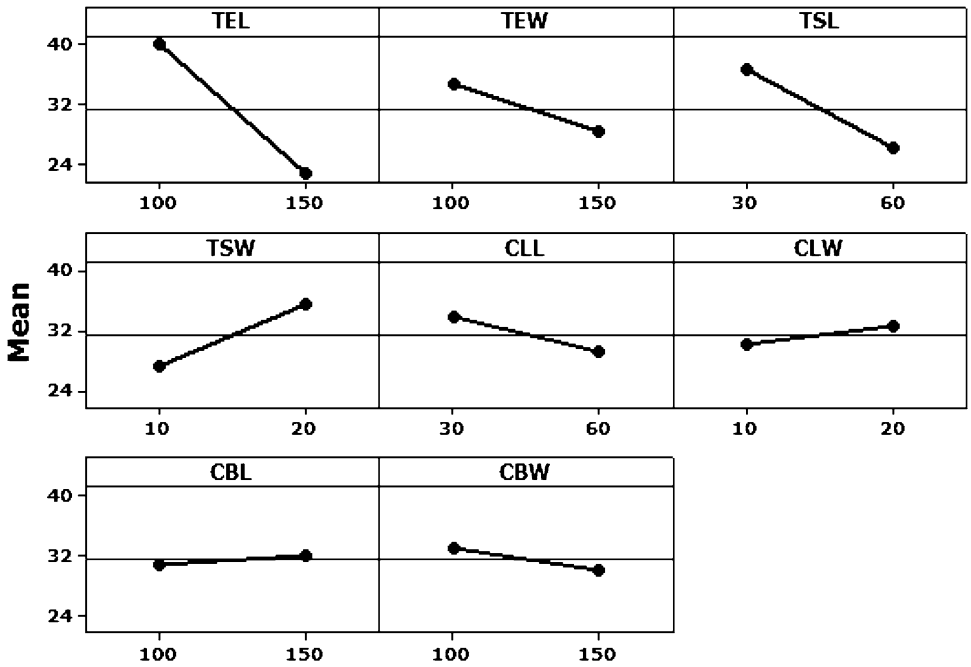

Fig. 2 Mean effect plot of the factors for the pull-in voltage

and when the group mean at the factor levels are equal to the overall mean then the sum of the factor level effects becomes zero. It shows that when the means for each of the factor levels of a factor are equal, then there is no effect of that particular factor on the output response. Figure 2 shows the mean effect plot of the control factors for the output response.

3.3.2 Estimation of parameters

Total variability in the output response for each factor is measured in the form of the total sources of variance SS_T and it is combination of factor sum of squares (factor effects) SS_A and error sum of squares (random error) SS_E. These values are computed as:

$$SS_A = \sum_{i=1}^{a} \sum_{j=1}^{n_i} (\bar{y}_i - \bar{y})^2 \tag{3}$$

$$SS_E = \sum_{i=1}^{a} \sum_{j=1}^{n_i} (y_{ij} - \bar{y}_i)^2 \tag{4}$$

$$SS_T = SS_A + SS_E \tag{5}$$

where $\bar{y}_i$ is the factor level group mean, $\bar{y}$ is the overall mean, a is the number of levels of the factor, y_{ij} is the the j th response in the ith factor level and n_i is the number for which the factor is at level i.

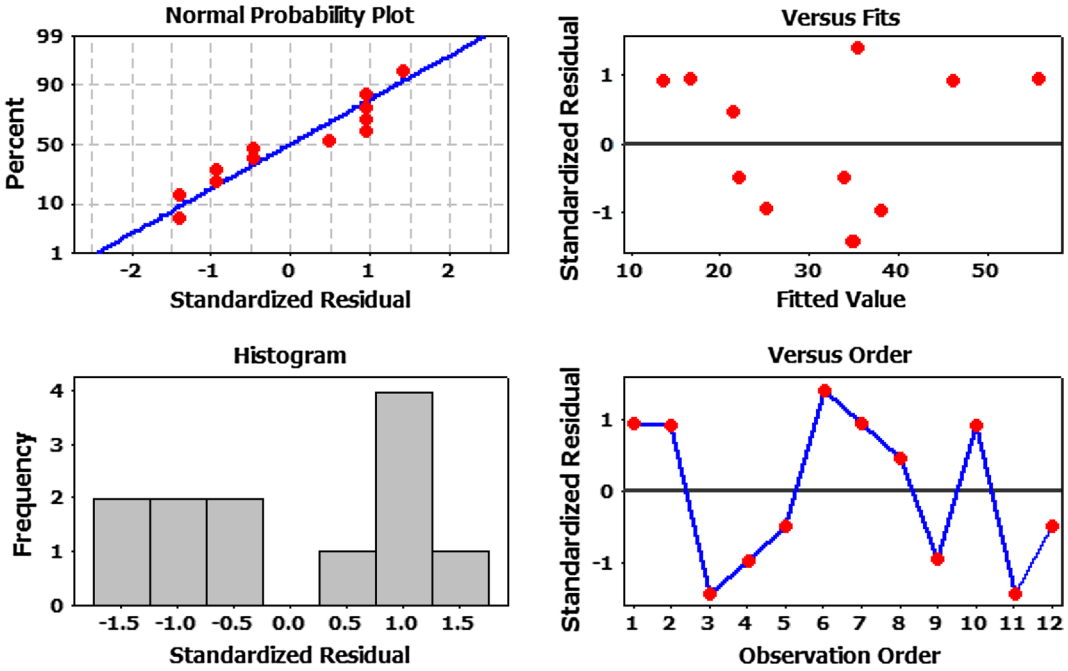

Fig. 3 Residual plots for the Placket–Burman matrix data

3.3.3 Validity of ANOVA assumptions

ANOVA is based on the following two assumptions:

1. The values for each factor level follow a normal distribution.
2. The variances are the same for each factor level.

It is observed that the researchers rarely verify the validity of these assumptions which results in an analysis non-robust to the assumption violations. Though mild deviation from normality and heterogeneity in variance can be tolerated for equal group sizes, yet it is highly advisable to explore the extent to which violations are present in the design. Montgomery (1997) has proposed that the basic assumptions can be verified by examining the residuals e_{ij} given by:

$$e_{ij} = y_{ij} - \hat{y}_{ij} \tag{6}$$

where $\hat{y}_{ij} = \hat{\mu} + \hat{\alpha}_i = \bar{y} + (\bar{y}_i - \bar{y}) = \bar{y}_i$ is the estimate of any observation in the ith factor level and is the corresponding factor level average. Normality assumption can be verified by analyzing the normal probability plot and a histogram of residuals. If the normality assumption on the residuals is verified the histogram should resemble the normal distribution and normal probability plot of residuals should follow the straight line. The assumption of equal variance can be verified by visualizing the plot of residuals vs. fitted value. If the plot is structureless then it is assumed that the variances are same for each level of the factor. Figure 3 shows residual plots for the pull-in voltage obtained using the Plackett–Burman design matrix, given in Table 2.

In the plot standardized residuals are used instead of ordinary residuals. Standardized residuals d_i help to identify the outliers in the data and are calculated by:

$$d_i = \frac{e_{ij}}{\sqrt{MS_E}} \tag{7}$$

where $\sqrt{MS_E}$ is the mean error sum of squares. In Fig. 3 standardized residuals lie in the interval $-3 \leq d_i \leq 3$, thus rejecting the possibility of any outliers.

3.3.4 Statistical tests for normal distribution and homogeneity of variance

Though a visual inspection of the residual plots give an idea of the normality and homogeneous variance assumptions violations, but they fail to provide a conclusive evidence. There are good number of tests available for the both assumptions verification in literature (Razali and Wah 2011). Generally, empirical distribution function (EDF) based tests like Anderson–Darling, Kolmogorov–Smirnov and Cramer–von Mises tests are used for the test of the normality distribution. For the variance homogeneity analysis, Bertlett's test and Levene's test are generally carried out (Montgomery 1997). Leven's test, for its robustness to the non normality as compared to Bertlett's test, is preferred for the non normal distributions.

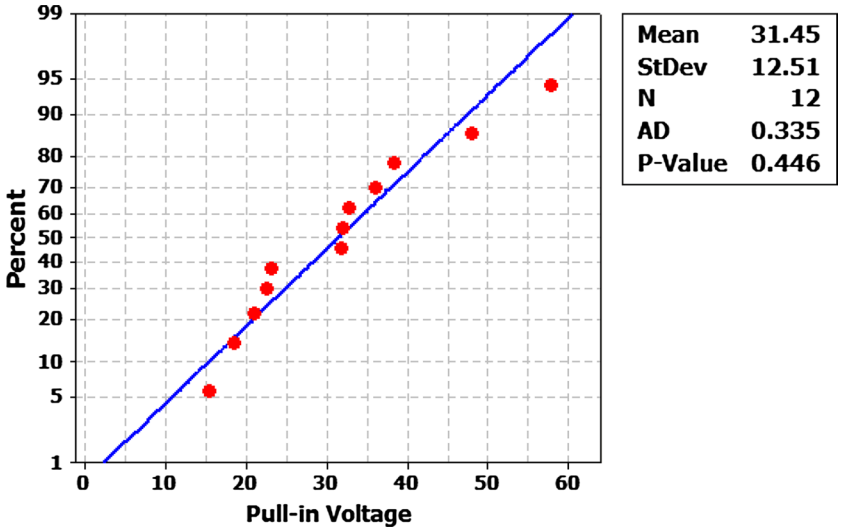

Fig. 4 Normal probability plot based on the Anderson–Darling test

To verify the normality assumption Anderson–Darling test is used in our work (Anderson and Darling 1954). According to Stephens (1976), this test is the most powerful EDF test. Anderson–Darling test conduct a statistical test on the hypothesis to find out if the distribution curve is normal or not. If p value <0.05, then it is said with 95 % confidence level that the data comes from the non normal distribution. However, for p value ≥0.05 distribution curve is assumed normal. Figure 4 shows that the p value obtained using Anderson–Darling is 0.446 > 0.05, satisfying the condition for normal distribution.

Next, Leven's test is carried out for verification of the homogeneity of variance assumption. Leven's test uses the absolute deviation of the observation y_{ij} in each factor level from the factor level group median. Based on these calculations, it tests the null-hypothesis of equal variance between the factor levels of a factor. If the resulting p value <0.05, it rejects the null-hypothesis and states that the variances for the factor level groups are different. If p value ≥0.05 it fails to reject the null-hypothesis and it is assumed with 95 % confidence level, that variances for the factor level groups are equal. Leven's test is carried out for the eight two level factors TEL, TEW, TSL, TSW, CCL, CLW, CBL and CBW. Figure 5 shows the Leven's plot for deviation for each factor along with the obtained p value. It is observed that the p value for all the eight factors is greater than 0.05 thus verifying the condition for homogeneity of variance.

3.3.5 *ANOVA results for the screening Plackett–Burman design*

Significant factors affecting the output response can be obtained by using ANOVA based F-test. This test investigates the following hypothesis for each factor:

$$\left.\begin{array}{l} H_o : \mu_1 = \mu_2 = \cdots = \mu_a \\ H_1 : \mu_i \neq \mu_j \quad \textit{for atleast one pair } (i,j) \end{array}\right\} \tag{8}$$

The F value is obtained by:

$$F_o = \frac{SS_A/a-1}{SS_E/N-a} = \frac{MS_A}{MS_E} \tag{9}$$

where $(a-1)$ is the degrees of freedom for the factor A, $(N-a)$ is the error degrees of freedom, MS_A and MS_E are the mean sum of squares and error sum of squares for the factor A respectively. The null hypothesis is rejected if F_o is greater than the critical value $F_{\alpha,a-1,N-a}$, where α is the level of significance. Critical values are obtained using tables for F-distribution with different significance levels. Table 3 shows the analysis of variance for the eight factors with their respective F and p values. The factor significance of 95 % level (p value <0.05) is considered to screen out the significant factors affecting the output response. A p value <0.05 is the probability that the obtained F value is not due to any random variation and is attributed to the difference in means between two factor levels of a factor. Results show that the TEL, TEW, TSL and TSW are the most significant factors.

The results obtained using ANOVA are confirmed using pareto charts (Ishikawa 1976) and half normal probability plots (Daniel 1959). Pareto charts sort and plot the square effects expressed as percentage of sum of all square effects. Half normal probability plots give graphical representation of normal probabilities versus coefficient estimates. The estimates for the significant factors depart from the fitted line as they do not follow the normal distribution of error. Figure 6a, b shows the half-normal plot and pareto plot for the eight factors respectively, showing TEL, TEW, TSL and TSW to be most significant factors at 95 % confidence level.

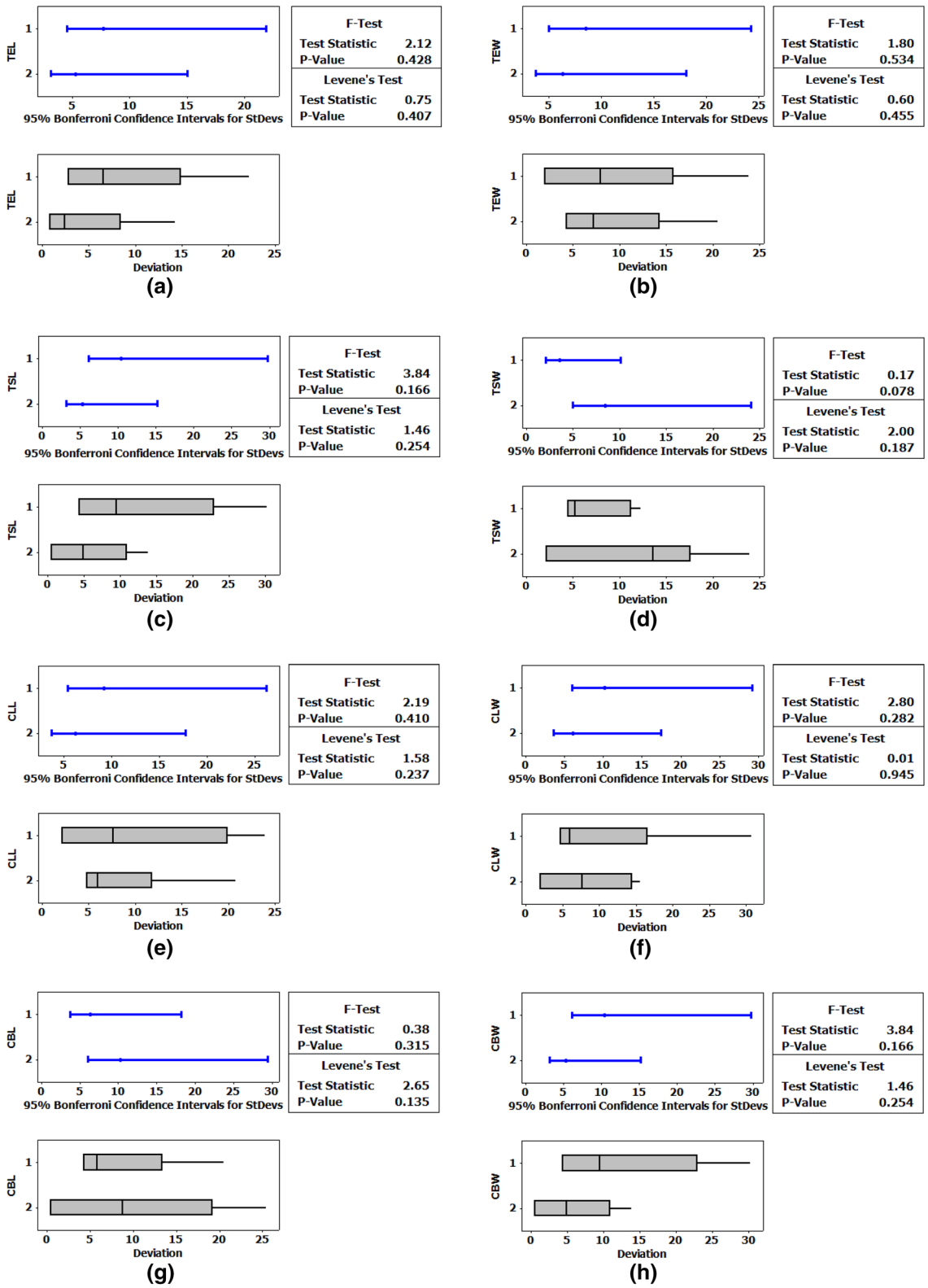

Fig. 5 Leven's deviation plot for **a** TEL, **b** TEW, **c** TSL, **d** TSW, **e** CLL, **f** CLW, **g** CBL, **h** CBW

Table 3 Analysis of variance for the Plackett–Burman design

Code	Control factors	DF	Sum of squares	Mean square	F ratio	p value
	Main effects	8	1,730.8	216.35	12.24	0.031
X_1	TEL	1	904.80	904.80	51.21	0.006
X_2	TEW	1	181.99	181.99	10.3	0.048
X_3	TSL	1	322.85	322.85	18.84	0.023
X_4	TSW	1	198.45	198.45	11.23	0.044
X_5	CLL	1	64.40	64.40	3.65	0.152
X_6	CLW	1	18.25	18.25	1.03	0.384
X_7	CBL	1	4.80	4.80	0.27	0.638
X_8	CBW	1	25.23	25.23	1.14	0.318
	Residual error	3	53.01	17.669		
	Total	11	1,783.81			

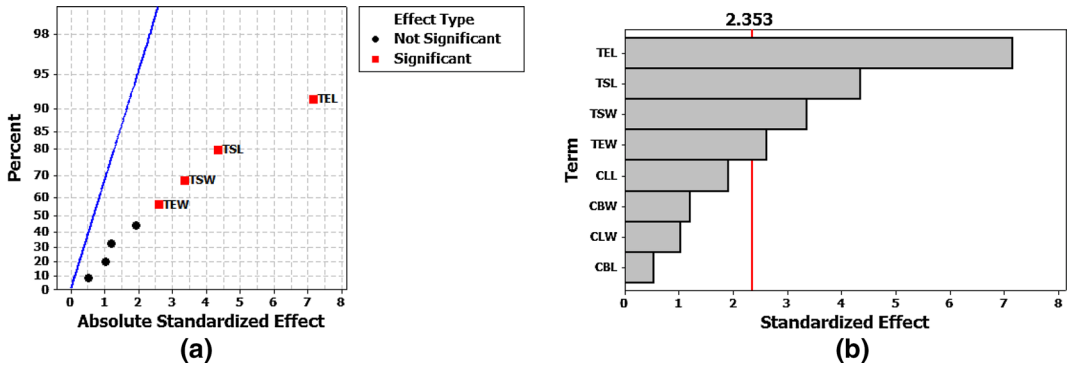

Fig. 6 **a** Half-normal probability plot and **b** Pareto chart for the significant factors

4 Response surface methodology

The significant factors (TEL, TEW, TSL, TSW), identified by Plackett–Burman based screening design are further explored by the response surface method. Response surface method uses a statistical and mathematical techniques to develop an empirically-based model of the observed response value (dependent variable), and number of associated factors (independent variables). General model of RSM is given by:

$$y = f'(x)\beta + \varepsilon \tag{10}$$

where $x = x_1, x_2, \ldots, x_k, f(x)$ is vector function of p elements that consists of the powers and cross products of power of $x_1, x_2, \ldots, x_k$ up to certain degrees represented by $d(\geq)1$, β is a vector of p unknown constant coefficients often referred as parameters and ε is random experimental error assumed to have zero mean. Output response y is measured for a series of n experiments with specific settings of the independent variables $x_1, x_2, \ldots, x_k$. The totality of these settings define the so called response surface design which is represented by a matrix of $n \times k$, called the design or model matrix, given by;

$$D = \begin{bmatrix} x_{11} & x_{12} & \ldots & x_{1k} \\ x_{21} & x_{22} & \ldots & x_{2k} \\ \vdots & & \ddots & \vdots \\ x_{n1} & a_{n2} & \ldots & x_{nk} \end{bmatrix} \tag{11}$$

where x_{ui} denotes the uth design setting of x_i $(i = 1, 2, \ldots, k : u = 1, 2, \ldots, n)$. Each row of D represents a point, referred as a design point in a k-dimensional Eculidean space. For the y_u being the response value obtained as a result of applying the uth setting of x, namely $x_u = (x_{u1}, x_{u2}, \ldots, x_{uk})$, $(u = 1, 2, \ldots, n,)$, Eq. 10 is given as.

$$y_u = \acute{f}(x_u)\beta + \varepsilon_u \tag{12}$$

where ε_u denotes the error term at the uth experimental run. Equation (12) in matrix form can be expressed as;

$$Y = X\beta + \varepsilon. \tag{13}$$

Assuming that ε has zero mean and variance-covariance matrix, the ordinary least square estimator of β is given by;

$$\hat{\beta} = (XX)^{-1}XY. \tag{14}$$

Table 4 Analysis of variance for the Plackett–Burman design

Code	Control factors	Low level (−1)	Medium level (0)	High level (+1)
X_1	TEL	100	125	150
X_2	TEW	100	125	150
X_3	TSL	30	45	60
X_4	TSW	10	15	20

Method of least squares regression is used to estimate the parameters β_0, β_1, β_{ii} and β_{ij}, so that the sum of squares of the predicted values, $\hat{y}(x)$, from the actual values, $y(x)$, are minimized.

4.1 Box–Behnken design

Table 4 shows the three different levels low (−1), medium (0) and high (+1) for the four significant factors TEL, TEW, TSL and TSW. Complete Box–Behnkin design matrix for the four factors with 27 experimental runs and the output response, obtained through ANSYS simulations, is shown in Table 5. The other variables CLL, CLW, CBL and CBW are maintained at a constant level which gave minimum pull-in voltage in the Plackett–Burman screening design. Polynomial equation obtained, considering second order model and calculating the value of the estimators, is given as;

$$\left.\begin{aligned} Y &= 27.2 - 7.38X_1 - 2.72X_2 - 5.208X_3 + 4.12X_4 \\ &\quad + 0.40X_1^2 + 0.19X_2^2 + 0.20X_3^2 - X_4^2 \\ &\quad + 0.825X_1X_2 + 1.30X_1X_3 - 0.925X_1X_4 \\ &\quad + 0.425X_2X_3 + 0.40X_2X_4 - 1.15X_3X_4 \end{aligned}\right\} \quad (15)$$

4.2 Regression significance analysis of Box–Behnken design

The significance of regression is used to determine if there is a relationship between the response variable y and the subset of independent variables $x_1, x_2, \ldots, x_k$ (Montgomery 1997). The procedure requires that the errors ε in the model be normally distributed with mean zero and variance σ^2. These assumptions are verified by using residual plots. The residual in regression analysis is defined as the difference between the observation value y_i and the fitted value $\hat{y}_i$. Figure 7 shows the residual plots for the Box–Behnkin design. It can be observed that normal probability and histogram plots show a distribution close to normal, and non-random pattern on fitted value versus standardized residuals plot suggests that the variance of the original observations is constant for all values of y. As the residuals plots clearly depict the normality and equal variance assumptions being satisfied, so the option for the further statistical tests can be ignored.

Table 5 Box–Behnkin design matrix and the output response for the 27 experimental runs

Run no.	X_1	X_2	X_3	X_4	Pull-in voltage (V)
1	0	+1	+1	0	19.5
2	+1	0	0	−1	16.4
3	+1	0	+1	0	16.8
4	0	−1	−1	0	35.6
5	0	+1	−1	0	29.4
6	−1	0	0	+1	38.5
7	0	0	+1	−1	18.4
8	−1	−1	0	0	38.4
9	0	0	+1	+1	24
10	0	+1	0	+1	27.8
11	0	−1	0	+1	34
12	−1	0	−1	0	44
13	+1	0	0	+1	22.2
14	0	0	0	0	27.2
15	0	−1	0	−1	24
16	+1	0	−1	0	24.8
17	+1	−1	0	0	21.5
18	−1	0	0	−1	29
19	−1	0	+1	0	28.8
20	0	+1	0	−1	19.4
21	0	0	0	0	27.2
22	0	−1	+1	0	24
23	+1	+1	0	0	17.6
24	0	0	0	0	27.2
25	−1	+1	0	0	31.2
26	0	0	−1	+1	36.2
27	0	0	−1	−1	36

The test for the regression is based on the following hypothesis;

$$\left.\begin{aligned} &H_o : \beta_1 = \beta_2 = \cdots = \beta_k \\ &H_1 : \beta_j \neq 0 \quad (\textit{for atleast one } j) \end{aligned}\right\}. \quad (16)$$

If null hypothesis is rejected it means that at least one of the independent variable significantly contributes to the model. This approach is similar to the ANOVA discussed in Sect. 3.3. Total sum of squares SS_{Total} in design are divided into sum of squares due to regression $SS_{Regression}$ and sum of squares due to residuals $SS_{Residuals}$ given as;

$$SS_{Total} = SS_{Regression} + SS_{Residuals} \quad (17)$$

where $SS_{Regression} = \hat{\beta}XY - \frac{\sum_{i=1}^{n} y_i^2}{n}$, $SS_{Residuals} = YY - \hat{\beta}XY$ with n equal to total number of experimental runs. The F-test ratio for the regression analysis is given as:

$$F_o = \frac{SS_{Regression}/k}{SS_{Residuals}/n-k-1} = \frac{MS_{Regression}}{MS_{Residuals}} \quad (18)$$

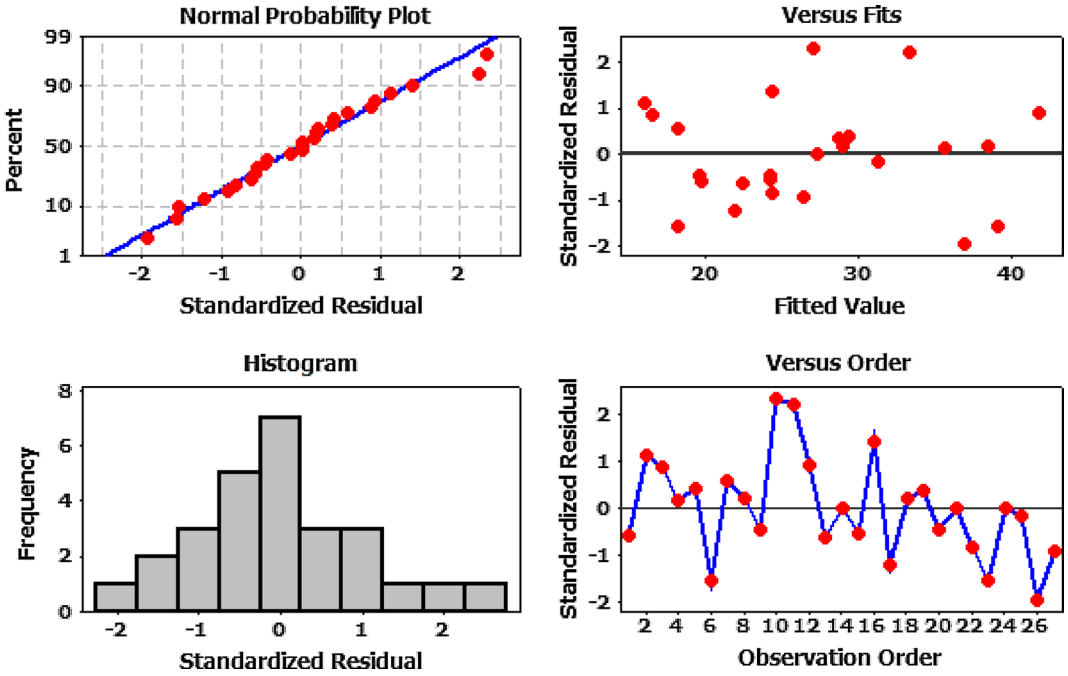

Fig. 7 Residual plots for the Box–Behnken design matrix data

where k is the number of independent variables. If the calculated $F_0 > F_{\alpha,k,n-k-1}$ (or p value $< \alpha$), then null hypothesis is rejected. In regression analysis coefficient of multiple determination R^2 is used as an indicator of model fit for a dependent variable. It explains how strongly the independent variables as a group are related to the dependent variable. The coefficient of multiple determination is calculated as;

$$R^2 = \frac{SS_{Regression}}{SS_{Total}}. \tag{19}$$

Since the value of R^2 increases even if the undesired terms are added, an alternative adjusted R^2 statics are generally used given by;

$$R^2_{adj} = 1 - \frac{SS_{Residuals}/(n-k-1)}{SS_{Total}/(n-1)}. \tag{20}$$

Table 6 shows the results of the regression analysis for the for independent variables X_1, X_2, X_3 and X_4 representing the factors TEL, TEW, TSL and TSW respectively. The model F value of 328.52, shows that the model is significant and there is <0.01 % chance that the model F value could have occurred due to random noise. High value of R^2 implies that there is an excellent correlation between the experimental and predicted values. Small difference between R^2 and R^2_{adj} shows that probability of having non-significant terms added in the model is negligible.

Table 6 Regression analysis for the Box–Behnkin design matrix regression model

Source	DF	Sum of squares	Mean square	F value	p value
Regression	14	1,301.54	92.967	328.52	<0.0001
X_1	1	654.16	654.16	2311.34	<0.0001
X_2	1	88.56	88.56	312.96	<0.0001
X_3	1	325.52	325.52	1150.31	<0.0001
X_4	1	204.19	204.19	721.55	<0.0001
X_1X_2	1	2.72	2.72	9.62	0.009
X_1X_3	1	6.76	6.76	23.89	<0.0001
X_1X_4	1	3.42	3.42	12.09	0.005
X_2X_3	1	0.72	0.72	2.55	0.136
X_2X_4	1	0.64	0.64	2.26	0.158
X_3X_4	1	5.29	5.29	18.69	0.001
$\sum_{i=1}^{4} X_i^2$	4	9.55	2.387	8.44	0.002
Residual error	12	3.40	0.283		
Total	26	1,304.94			

$R^2 = 0.997$, $R^2_{adj} = 0.994$

5 Results and discussion

The p values <0.05 for the X_1X_2, X_1X_3, X_1X_4 and X_3X_4 show that there is a significant relationship between the TEL and TEW, TEL and TSL, TEL and TSW, TSL and TSW for the output pull in voltage. Figure 8a, b show the

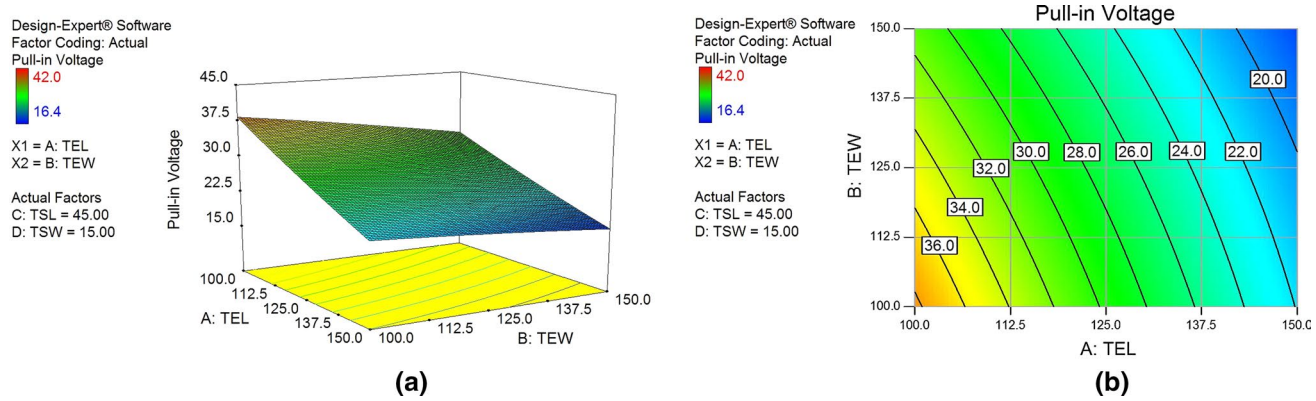

Fig. 8 **a** 3D surface plot, **b** contour plot for TEL and TEW for fixed values of TSL and TSW

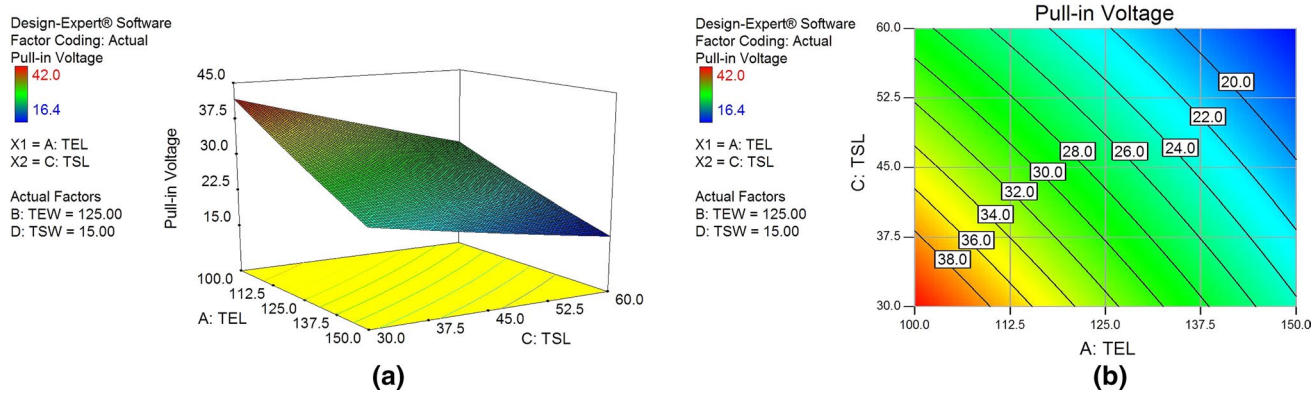

Fig. 9 **a** 3D surface plot, **b** contour plot for TEL and TSL for fixed values of TEW and TSW

3D surface plot and contour plot respectively, for the effect of TEL and TEW width at the medium values for the TSL and TSW. It shows that the pull-in voltage decreases with the increase in the TEL and TEW dimensions. Moreover, pull-in voltage is more sensitive to the TEL dimensions as compared to the TEW dimensions. With TEL = 150μm, the change in pull-in voltage due to TEW dimensions variations is very small. Figure 9a, b shows that the pull-in voltage has comparable sensitivity to both TEL and TSL when TEW and TSW are at their medium levels. Pull-in voltage decreases with the increase in both TEL and TSL dimensions. When the TEL > 125μm and TSL > 45μm then change in the pull-in voltage is relatively less sensitive to the change in TEL and TSL dimensions. Moreover, when the TEL = 150μm, the change in pull-in voltage is less effected for TSL > 45μm. Figure 10a, b shows that the pull-in voltage decreases with the increase in the TEL and decrease in the TSW dimensions. Pull-in voltage is more sensitive to the TSW variation for TEL < 125μm and this sensitivity decreases significantly for TEL > 140μm. Figure 11a, b shows that increasing the TSL length and decreasing the TSW decreases the pull-in voltage and for TSL > 45μm, the pull-in voltage is relatively less sensitive to the change in the TSW.

The results obtained by contour and surface plot analysis are further verified through optimization of the switch design with the objective; pull-in voltage ≤15 V with compact device dimensions. Table 7 shows the best four optimized solutions predicted by the developed RSM model. These results show that the observation number 3 with pull-in voltage of 14.29 V is most optimized design within the optimization criterion set. Figure 12 shows the optimization plots for pull-in voltage with TSL at 45 and 60μm respectively. The colored area shows the possible combinations of the parameters that result in pull-in voltage ≤15 V. The results are obtained using the statistical tool Design-Expert.

The RSM predicted pull-in voltage of 14.29 V, with 95 % prediction interval of $12.07 \leq V \leq 16.48$ for the optimal levels of the design parameters, is verified using FEM simulations. The value obtained by the FEM simulation

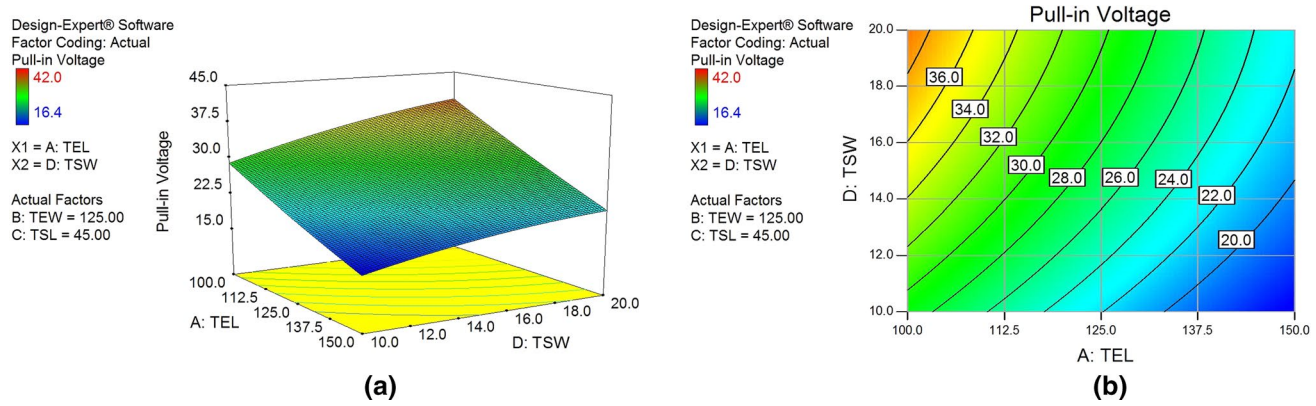

Fig. 10 **a** 3D surface plot, **b** contour plot for TEL and TSW for fixed values of TEW and TSL

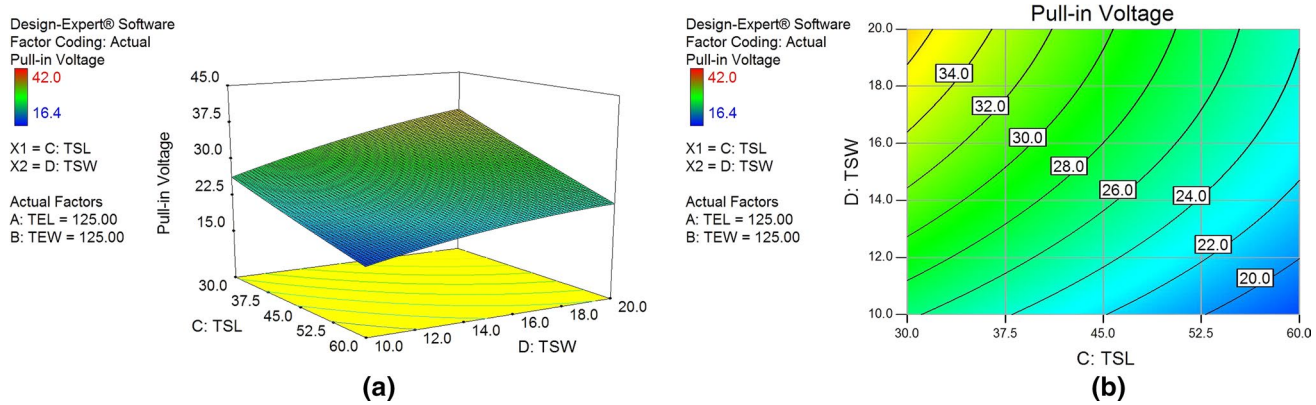

Fig. 11 **a** 3D surface plot, **b** contour plot for TSL and TSW for fixed values of TEL and TEW

Table 7 Predicted pull-in voltage for four different combinations of TEW and TSL with TEL = 150 μm and TSW =10 μm

Observation no.	TEL (μm)	TEW (μm)	TSL (μm)	TSW (μm)	Pull-in voltage (V)
1	150	100	45	10	17.28
2	150	150	45	10	14.37
3	150	100	60	10	14.29
4	150	150	60	10	12.22

is 16.2 V, which is close to the RSM predicted value and lies within the prediction interval. Figure 13a, b show the optimized design and the pull-in voltage obtained through ANSYS simulations.

Table 3 and Fig. 2 show that the CBW has negligible effect on the pull-in voltage at two different levels, so to keep the design dimensions compact, CBW with 150 μm (level 2) can be replaced with 100 μm (level 1) without considerably affecting the pull-in voltage. This is verified by FEM simulation. Figure 14 shows the modified optimized design with the corresponding pull-in voltage showing a negligible difference in the results as compared to the optimized design shown in Fig. 14.

Farinelli et al. (2008) have proposed an analytical expression for the pull-in voltage of STS design given by;

$$V_{pull\text{-}in} = \sqrt{\frac{E}{2.3911\varepsilon_o TEW}\left(\frac{g}{TEL}\right)^3\left(\frac{C}{(1-\nu)}\frac{TSWh_t^3}{TSL}+\frac{TEL}{CLL^2}\frac{CLWh^3}{6}\right)} \quad (21)$$

where E is the Young's modulus, ν is the Poisson's ratio and TSL, h_t, TSW, CCL, h and CLW are the length, height and width of the torsion spring and connecting lever, respectively. This relation shows that the CBL and CBW have no effect on the pull-in voltage confirming the results of the Plackett–Buram screening design. Moreover, this relation shows that the CLL and CLW also have effect on the pull-in voltage along with other parameters. Considerable slope of the line in mean effect plot in Fig. 2 shows that the CLL and CLW also affect the pull-in voltage and pull-in voltage

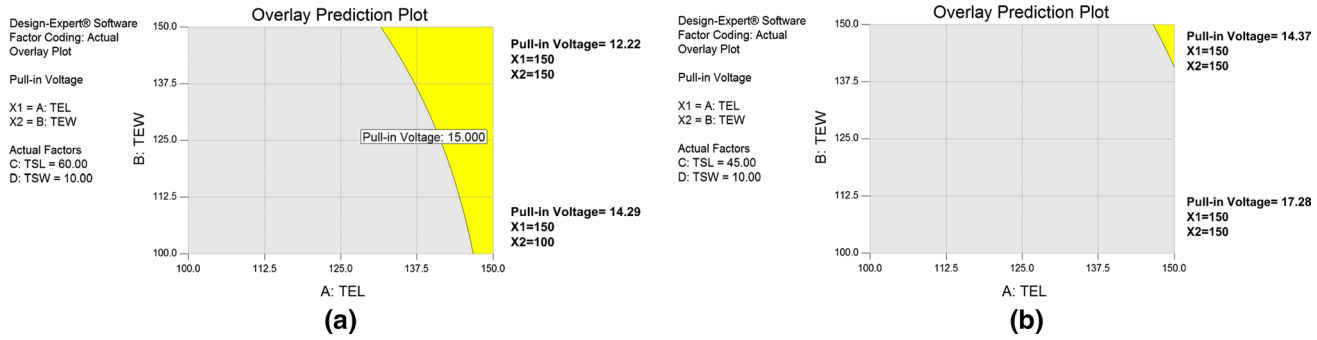

Fig. 12 **a** Optimization plot for TSL = 60 μm and TSW= 10 μm. **b** Optimization plot for TEL = 45 μm and TSW= 10 μm

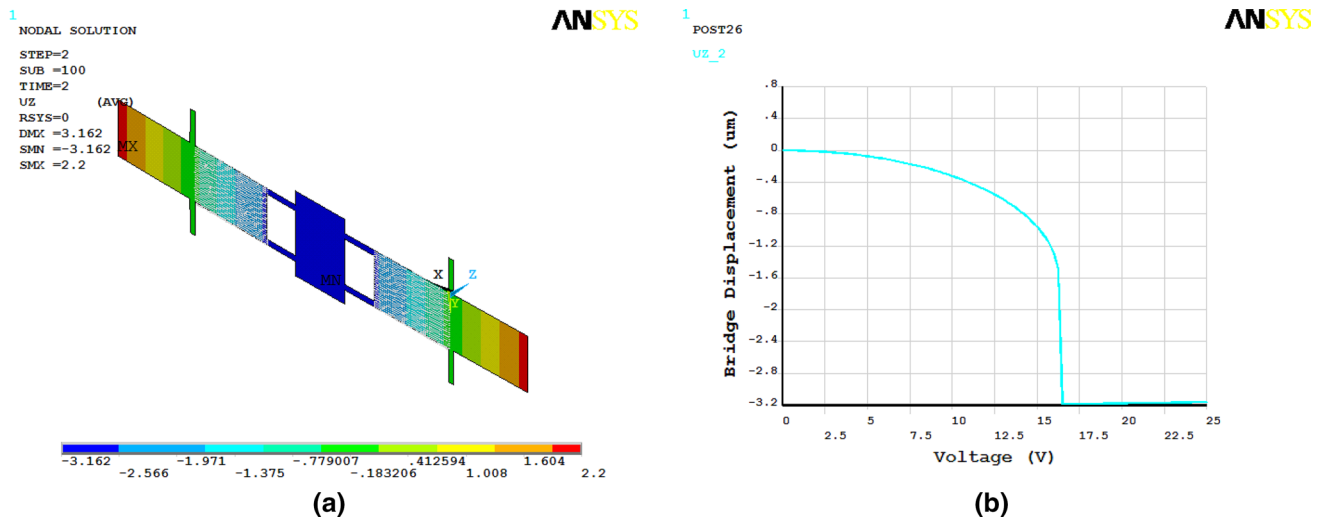

Fig. 13 **a** Displacement response for the optimized design. **b** Pull-in voltage for the optimized design

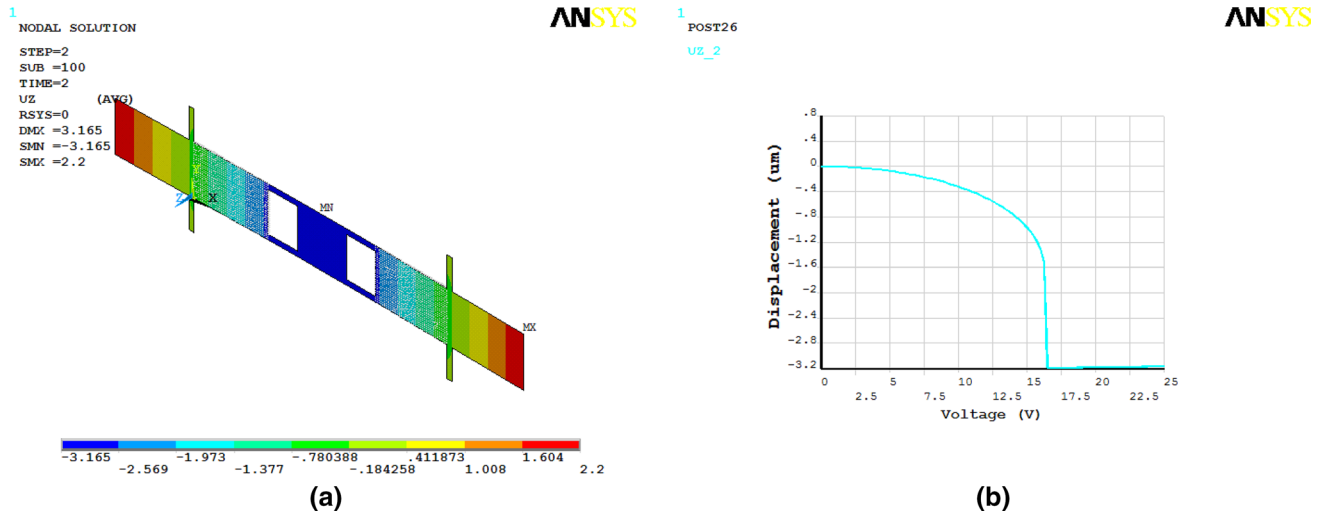

Fig. 14 **a** Displacement response for the modified optimized design. **b** Pull-in voltage for the modified optimized design

decreases with increasing the *CLL* and increasing the *CLW*, confirming the relation shown in Eq. (21). Though *CLL* and *CLW* are not shown significant as compared to other parameters with 95 % confidence level, these factors can be included in response surface methodology by lowering the confidence level.

6 Conclusion

The possibility of implementing DOE based design optimization for MEMS devices is presented. Symmetrical toggle RF MEMS switch design is optimized for the pull-in voltage using Plackett–Burman based fractional factorial design and Box–Behnken based response surface methodology. The design is optimized to achieve pull-in voltage $\leq$15 V with compact dimensions. Results obtained, using DOE technique, are verified through FEM based simulations and analytical results presented in literature, which showed a close agreement. The results suggested that statistical DOE based methodology for MEMS devices offers an efficient and feasible alternative approach for the optimization of MEMS devices with complex geometries.

References

Anderson TW, Darling DA (1954) A test of goodness of fit. J Am Stat Assoc 49(268):765–769

Ballestra A, Brusa E, De Pasquale G, Munteanu MG, Somá A (2008) RF-MEMS beam components: FEM modelling and experimental identification of pull-in in presence of residual stress. In: Design, test, integration and packaging of MEMS/MOEMS, pp 232–235

Benmessaoud M, Nasreddine MM (2013) Optimization of MEMS capacitive accelerometer. Microsyst Technol 19:713–720

Bouchaud J, Knoblich B (2007) RF MEMS switches deliver on early promise. Sens Transducers J 86:1802–1808

Box GE, Draper NR (1987) Empirical model-building and response surfaces. Wiley, New York

Daniel C (1959) Use of half-normal plots in interpreting factorial two-levels experiments. Technometrics 1:311–341

De Pasquale G, Veijola T, Somá A (2010) Modelling and validation of air damping in perforated gold and silicon MEMS plates. J Micromechanic Microengineering 20(1):015010

Farinelli P, Solazzi F, Calaza C, Margesin B, Sorrentino R (2008) A wide tuning range MEMS varactor based on a toggle push-pull mechanism. In: Microwave conference, pp 1501–1504

Ferreira SC, Bruns RE, Ferreira HS, Matos GD, David JM, Brandão GC, Dos Santos WL (2007) Box–Behnken design: an alternative for the optimization of analytical methods. Anal Chim Acta 597(2):179–186

Giacomozzi F, Calaza C, Colpo S, Mulloni V, Collini A, Margesin B, Farinelli P, Casini F, Marcelli R, Monnocchi G, Vietzorreck L (2008) Development of high con coff ratio RF MEMS shunt switches. Rom J Inf Sci Technol 11(2):143–151

Hamada M, Wu C (2000) Experiments: planning, analysis, and parameter design optimization. Wiley, New York

Ishikawa K (1976) Guide to quality control. Asian Productivity Organization. Nordica International, Hong Kong

Lee Y, Filipovic DS (2005) ANN based electromagnetic models for the design of RF MEMS switches. Microw Wirel Compon Lett IEEE 15(11):823–825

Lee Y, Park Y, Niu F, Filipovic D (2006) Design and optimisation of one-port RF MEMS resonators and related integrated circuits using ANN-based macromodelling approach. IEE Proc-Circuits Devices Syst 153(5):480–488

Liu Y, Yang HY, Wang GC (2012) Genetic algorithm based multidisciplinary design optimization of MEMS accelerometer. Appl Mech Mater 101:530–533

Maninder K, Rangra KJ, Kumar D, Singh S (2009) Parametric optimization of symmetric toggle RF MEMS switch for X-band applications. Int J Recent Trends Eng 2(7):95–98

Mason RL, Gunst RF, Hess JL (2003) Statistical design and analysis of experiments: with applications to engineering and science, vol 474. Wiley, New York

Montgomery DC (1997) Design and analysis of experiments, 5th edn. Wiley, New York

Mukherjee T, Iyer S, Feeder GK (1998) Optimization-based synthesis of microresonators. Sens Actuators A Phys 70(1):118–127

Plackett RL, Burman JP (1946) The design of optimum multifactorial experiments. Biometrika 33(4):305–325

Pramanik C, Saha H, Gangopadhyay U (2006) Design optimization of a high performance silicon MEMS piezoresistive pressure sensor for biomedical applications. J Micromechanics Microengineering 16:2060–2066

Rangra K, Margesin B, Lorenzelli L, Giacomozzi F, Collini C, Zen M, Soncini G, Tin L, Gaddi R (2005) Symmetric toggle switch-a new type of RF MEMS switch for telecommunication applications. Design and fabrication. Sens Actuators A 123–124:505–514

Razali NM, Wah YB (2011) Power comparisons of Shapiro–Wilk, Kolmogorov–Smirnov, Lilliefors and Anderson–Darling tests. J Stat Model Anal 2(1):21–33

Rebeiz GM, Entesari K, Reines IC, Park SJ, El-Tanani MdA, Grichener A, Brown AR (2009) Tuning in to RF MEMS. In: IEEE microwave magazine, pp 55–72

Rebeiz GM (2003) RF MEMS: theory, design and technology. Wiley, Hoboken

Stephens MA (1976) Asymptotic power of EDF statistics for exponentiality against Gamma and Weibull alternatives. Department of Statistics, Stanford University, Report No. 297

Wan W, Lowther DA (2007) Design and synthesis of wide tuning range variable comb drive MEMS capacitors. COMPEL Int J Comput Math Electr Electron Eng 26(3):689–699

Wang Z, Liu Z (2009) An analytical method for optimization of RF MEMS wafer level packaging with CPW detuning consideration. In: Progress in electromagnetics research symposium proceedings, Moscow, pp 479–483

Wilcock R, Kraft M (2011) Genetic algorithm for the design of electro-mechanical sigma delta modulator MEMS sensors. Sensors 11(10):9217–9232

Zhang Y, Kamalian R, Agogino AM, Séquin CH (2005) Hierarchical MEMS synthesis and optimization. In: Smart structures and materials, international society for optics and photonics, pp 96–106